Prognostic impact of the bone marrow tumor microenvironment, HLA-I and HLA-Ib expression in MDS and CMML progression to sAML

Marcus Bauer, Nadja Jäkel, Andreas Wilfer, Anja Haak, Markus Eszlinger, Katalin Kelemen, Monika Haemmerle, Haifa Kathrin Al-Ali, Barbara Seliger & Claudia Wickenhauser

View supplementary material ☐

Published online: 06 Mar 2024.

Submit your article to this journal ☐

Article views: 437

View related articles ☐

View Crossmark data ☐

Taylor & Francis
Taylor & Francis Group

ORIGINAL RESEARCH

OPEN ACCESS

Check for updates

Prognostic impact of the bone marrow tumor microenvironment, HLA-I and HLA-Ib expression in MDS and CMML progression to sAML

Marcus Bauer[a], Nadja Jäkel[b], Andreas Wilfer[a,c], Anja Haak[a], Markus Eszlinger[a], Katalin Kelemen[a], Monika Haemmerle[a], Haifa Kathrin Al-Ali[b,c], Barbara Seliger[d,e,f], and Claudia Wickenhauser[a]

[a]Institute of Pathology, University Hospital Halle, Martin Luther University Halle-Wittenberg, Halle, Germany; [b]Department of Hematology, University Hospital Halle, Martin Luther University Halle-Wittenberg, Halle, Germany; [c]Krukenberg Cancer Center Halle, University Hospital Halle, Martin Luther University Halle-Wittenberg, Halle, Germany; [d]Medical Faculty, Martin Luther University Halle-Wittenberg, Halle, Germany; [e]Medical Faculty, Fraunhofer Institute for Cell Therapy and Immunology, Leipzig, Germany; [f]Institute of Translational Immunology, Medical School "Theodor Fontane", Brandenburg an der Havel, Germany

ABSTRACT

Genetic aberrations and immune escape are fundamental in MDS and CMML initiation and progression to sAML. Therefore, quantitative and spatial immune cell organization, expression of immune checkpoints (ICP), classical human leukocyte antigen class I (HLA-I) and the non-classical HLA-Ib antigens were analyzed in 274 neoplastic and 50 non-neoplastic bone marrow (BM) biopsies using conventional and multiplex immunohistochemistry and correlated to publicly available dataset. Higher numbers of tissue infiltrating lymphocytes (TILs) were found in MDS/CMML (8.8%) compared to sAML (7.5%) and non-neoplastic BM (5.3%). Higher T cell abundance, including the CD8^{+} T cell subset, inversely correlated with the number of pathogenic mutations and was associated with blast BM counts, ICP expression, spatial T cell distribution and improved patients' survival in MDS and CMML. In MDS/CMML, higher PD-1/PD-L1/PD-L2 and HLA-I, but lower HLA-G expression correlated with a significantly better patients' outcome. Moreover, a closer spatial proximity of T cell subpopulations and their proximity to myeloid blasts showed a stronger prognostic impact when compared to TIL numbers. In sAML – the continuum of MDS and CMML – the number of TILs had no impact on prognosis, but higher CD28 and HLA-I expression correlated with a better outcome of sAML patients. This study underlines the independent prognostic value of the tumor microenvironment in MDS/CMML progression to sAML, which shows the most pronounced immune escape. Moreover, new prognostic markers, like HLA-G expression and spatial T cell distribution, were described for the first time, which might also serve as therapeutic targets.

Introduction

Myeloid neoplasms (MN) comprise heterogeneous clonal hematologic malignancies including among others, myelodysplastic neoplasms (MDS), myeloproliferative neoplasms (MPN) and myelodysplastic/myeloproliferative neoplasms (MDS/MPN) with chronic myelomonocytic leukemia (CMML).[1,2] These diseases greatly differ regarding clinical features, morphology, immunophenotyping, blood parameters, cytogenetics, molecular genetics and can be grouped a large number of subtypes,[1,2] but share a variable probability to progress to secondary acute myeloid leukemia (sAML), which genetically differs from de-novo AML (dnAML).[3,4] During the last years, genomic profiling increased the understanding of initiation and progression of MN and has improved the diagnostic accuracy and prognostic risk stratification. In recent years, it has been shown that inflammation plays a crucial role in MN pathophysiology,[5-8] which can be altered by genetic aberrations[9-12] and influences therapy resistance in AML.[13-15] Furthermore, immune-mediated cell death and significant alterations in the expression of immune checkpoint (ICP) molecules can occur throughout the course of

MN.[16,17] The ICP expression can be influenced by therapeutic interventions and its aberrant expression has been associated with a poor survival.[18] The treatment with hypomethylating agents (HMA) resulted in improved outcomes and prolonged survival of higher risk MDS, CMML and (s)AML patients,[19-21] which was associated with the induction of tumor antigen expression[22] as well as ICPs.[23-25] Moreover, the ICP upregulation upon HMA treatment provides a potential resistance mechanism in MN[23] and further suggests a combination of HMA with ICP inhibitors.[26]

Until now, there exists only limited information about the prognostic impact of the local tumor microenvironment (TME) in the bone marrow (BM) on the MN progression to sAML and its interrelationship with the mutational profile of MDS, CMML and sAML, respectively. Therefore, this study addressed the prognostic relevance of the quantity and spatial organization of the immune cell repertoire in the BM as well as the expression of immune response relevant molecules, which was analyzed in 274 BM biopsies (BMB) of patients with proofed MDS, CMML or sAML and 50 non-neoplastic BM (nnBM). The HLA-I, HLA-Ib and ICP expression were correlated to

a publicly available dataset of MDS samples and healthy controls. Moreover, the HLA-I, HLA-Ib and ICP expression of our cohort was correlated to the mutational profile, therapy and patients' outcome. These data provide information for optimization of (immuno-oncological) treatment strategies for MN.

Materials and methods

Patients' samples and ethics approval

Formalin fixed and paraffin embedded (FFPE) BMBs were collected between 2014 and 2022 and archived at the Institute of Pathology of the University Hospital Halle, Germany. The collective encompasses 50 nnBM, 106 MDS, 36 CMML and 132 sAML samples. The scientific use of the FFPE BMBs was approved by the Ethical Committee of the Medical Faculty, Martin-Luther University Halle-Wittenberg, Germany (2017–81 and 2023–196). Clinical data from these patients were available, such as age, sex, disease status, clinical risk score, therapy, available genetic data and survival time (Table 1). The following risk scores were applied: Revised International Prognostic Scoring System (IPSS-R) in MDS patients, CMML-specific Prognostic Scoring System (CPSS) in CMML patients, European LeukemiaNet (ELN) score in sAML patients. Progression-free survival (PFS) data of MDS and CMML patients were obtained with 3-year follow-up and referred to progression to sAML or disease-related death. In sAML patients, the overall survival (OS) was obtained.

Mutational analysis

20 ng DNA/sample was employed for next generation sequencing (NGS) library preparation according to the manufacturer's instructions. For NGS, three different NGS multigene panels with a broad overlap of genes examined were used (Supplementary Table S1) encompassing the most important and most frequently mutated genes in myeloid neoplasms. Samples from 2017 to 2019 were analyzed with the NEOmyeloid Panel (New Oncology, Siemens Healthineers, Erlangen, Germany), samples from 2019 to 2021 with the TruSight Myeloid Sequencing Panel (Illumina, San Diego, CA, USA) and cases from 2021 to 2022 with the VariantPlex Myeloid Panel (ArcherDX, Boulder, CO, USA). NGS was performed on a NextSeq/MiniSeq (Ilumina, San Diego, CA, USA) and the subsequent bioinformatics evaluation was carried out using the manufacturer's NGS platforms or the Seamless NGS platform (ecSeq Bioinformatics GmbH, Leipzig, Germany). Genomic variants/mutations were identified by a sequence homology comparison with the reference genome GRCh37/hg19 (NCBI - https://www.ncbi.nlm.nih.gov/grc/human). The nomenclature of variants/mutations is based on the recommendations of the Human Genome Variation Society (http://varnomen.hgvs.org/). All variants/mutations in the present study were reevaluated in 2022.

Standard morphological evaluation of the bone marrow and immunohistochemistry

Histopathological diagnosis was performed according to the diagnostic criteria of the World Health Organization (WHO) classification of Tumors of Hematopoietic and Lymphoid tissues, fourth edition 2017 and 2022.[27,28] For immunohistochemistry (IHC), all BMBs were stained with antibodies directed against the human leucocyte antigen (HLA) class I heavy chain (HC), HLA-E, HLA-F, HLA-G, CD34, CD117, MPO, lysozyme and CD71 according to the supplier's instructions. Further diagnostic information for the establishment of the diagnosis of a MN was taken from the Medical Records including cytology, cytogenetics and peripheral blood parameters.

Multispectral imaging

In order to analyze the spatial immune cell distribution of different immune cell subpopulations and the expression of ICP molecules, multispectral imaging (MSI) was performed as recently described[29] employing five different multiplex Ab panels as listed. Panel-1: CD3, CD8, FoxP3, MUM1p, CD34 and granzyme B (GrB); panel-2: CD3, CD34, PD-1, PD-L1 and PD-L2; panel-3: CD3, CD8, CD11c, cytotoxic T lymphocyte-associated protein 4 (CTLA-4), CD80 and CD86; panel-4: CD68, CD163, CD16, CD56, T cell immunoglobulin and mucin-domain containing-3 (TIM3) and galectin 9 (Gal-9); panel 5: CD3, LAG3, T cell immunoreceptor with Ig and ITIM domains (TIGIT), CD28, CD69 and CD33 (Supplementary Table S2). Briefly, after antigen retrieval the tissues were incubated for 30 min with the primary Ab followed by the secondary Ab (Akoya biosciences, Marlborough, MA, USA, Opal Polymer HRP Ms + Rb) for 10 min. Tyramide signal amplification (TSA) visualization was performed using the Opal seven-color IHC kit (Opal 520, Opal 540, Opal 570, Opal 620, Opal 650, Opal 690, Akoya biosciences) and DAPI. Stained slides were imaged employing the PhenoImager HT platform (Akoya biosciences, Marlborough, MA, USA). Cell segmentation and phenotyping were performed using the inForm software (PerkinElmer Inc.). The frequency of immune cell populations and their cartographic coordinates were evaluated using the R packages phenoptr and phenoptrReports packages (https://github.com/akoyabio).

Analysis of immune modulatory genes using publicly available RNA data

In order to compare the ICP as well as classical and non-classical HLA-I expression in MDS in comparison to healthy donors, a publicly available dataset (GSE30195)[30] containing Affymetrix Human Genome U133 Plus 2.0 Array data of purified BM CD34^{+} cells of untreated MDS patients and healthy controls was used. The differentially gene expression (DGE) of various ICP and HLA genes was determined by employing the Gene Expression Omnibus (GEO) repository (https://www.ncbi.nlm.nih.gov/geo/). DEG of MDS vs healthy controls was analyzed and visualized using the GEO2R tool (https://www.ncbi.nlm.nih.gov/geo/geo2r/).

Table 1. Clinical and immunological parameters.

	nnBM	MDS	CMML	sAML	total
number	50	106	36	132	324
age (mean)	20–87 (62)	25–86 (66)	31–86 (63)	26–80 (64)	20–87 (63)
sex (male/female)	29/21	58/48	19/17	80/52	186/138
diagnosis (n)	–	MDS-EB0 (52)	CMML-0 (11)	–	–
		MDS-EB1 (33)	CMML-1 (9)		
		MDS-EB2 (21)	CMML-2 (16)		
low clinical risk score	–	22.1	8.3%	42.4%	–
intermediate clinical risk score		40.0	66.7%	18.6%	
high clinical risk score		37.9	25.0%	39.0%	
HMA treatment (treated/untreated)	–	23/83	6/30	13/119	–
alloSCT (treated/untreated)	–	40/66	9/27	48/84	97/177
genetic data available	–	63	12	45	120
survival data available	–	80	25	111	216
HLA-I expression					
HLA-A,B,C HC H-score	190–300	110–300	70–300	10–300	10–300
(mean)	(238)	(214)	(184)	(179)	(197)
HLA-A,B,C HC^{high}	98.0%	49.1%	55.6%	45.5%	54.5%
HLA-E H-score	90–220	70–200	0–280	10–260	0–280
(mean)	(171)	(132)	(135)	(108)	(130)
HLA-F H-score	20–300	80–300	10–300	10–380	10–300
(mean)	(175)	(170)	(160)	(145)	(158)
HLA-G H-score	0–6	0–20	0–150	0–250	0–250
(mean)	(1.2)	(4.6)	(8.5)	(20)	(11.6)
immune cell infiltration (%)					
TIICs [mean]	13.1	17.1	24.9	16.8	18.5
TILs [mean]	5.3	8.9	8.6	7.5	7.3
T cells	0.0–11.9	0.5–26.1	0.3–22.1	0.0–51.1	0.00–51.1 (5.6)
(mean)	(4.9)	(7.8)	(6.9)	(5.9)	
CD3$^+$CD8$^+$ T cells	0.0–6.2	0.2–25.4	0.1–17.1	0.0–11.3	0.0–25.4 (4.5)
(mean)	(1.9)	(4.7)	(4.4)	(1.4)	
GrB$^+$ T and NK cells	0.0–3.8	0.1–24.1	0.1–10.2	0.0–18.4	0.0–24.1 (2.8)
(mean)	(1.4)	(3.6)	(2.9)	(2.5)	
CD3$^+$FoxP3$^+$ Tregs	0.0–0.8	0.0–5.5	0.0–7.6	0.0–3.7	0.0–6.7
(mean)	(0.18)	(0.5)	(0.5)	(1.6)	(1.4)
MUM1p$^+$ B/plasma cells	0.0–3.4	0.1–14.3	0.0–13.8	0.0–13.6	0.0–14.3 (1.7)
(mean)	(0.4)	(1.1)	(1.7)	(1.6)	
CD3$^-$CD56$^+$/CD16$^+$ NK cells	0.0–5.1	0.0–6.1	0.0–3.9	0.0–6.9	0.0–6.2
(mean)	(0.7)	(0.9)	(0.07)	(2.4)	(0.7)
CD11c$^+$ MCs	0.0–2.0	0.0–6.2	0.0–6.2)	0.0–0.8	0.0–4.2
(mean)	(0.2)	(0.3)	(1.6)	(0.9)	(0.7)
CD68$^+$CD163$^-$ macrophages	0.3–9.1	0.1–12.6	0.7–38.0)	0.0–18.7	0.0–18.7 (5.9)
(mean)	(6.2)	(4.4)	(8.1)	(3.6)	
CD68$^+$CD163$^+$macrophages	0.0–5.8	0.0–40.2	0.0–28.1	0.0–16.9	0.0–16.9 (3.9)
(mean)	(0.7)	(3.7)	(6.6)	(2.4)	
expression of immune checkpoint and immune cell activation marker (MFI & percentage of positive cells)					
LAG3 MFI [mean]	0.41	1.53	1.47	1.01	1.27
% [range (mean)]	0–66(14.3%)	0–100(49.9%)	0–99(33.9%)	0–98(25.1%)	0–100(35.4%)
TIGIT MFI [mean]	0.18	0.21	0.24	0.17	0.22
% [range (mean)]	0–53(9.1%)	0–60(3.6%)	0–35(5.3%)	0–89(7.1%)	0–89(5.6%)
TIM3 MFI [mean]	0.48	0.43	0.82	0.69	0.57
% [range (mean)]	2–27(4.8%)	1–99(43%)	3–97(40.5%)	0–99(65%)	0–89(49.7%)
Gal-9 MFI [mean]	0.22	0.41	0.84	0.18	0.39
% [range (mean)]	0.7–26(31.1%)	1–93(43.9%)	2–97(34.6%)	0–99(34.9%)	0–99(36.9%)
PD-L1 MFI [mean]	0.67	1.86	0.57	0.98	1.34
% [range (mean)]	0–21(8.3%)	0–99(41.9%)	0–97(13.8%)	0–98(20.2%)	0–99(24.1%)
PD-L2 MFI [mean]	0.87	1.11	1.24	1.39	0.84
% [range (mean)]	0–2(0.6%)	0–99(26.7%)	0–95(10.7%)	0–99(11.3%)	0–99(15.8%)
PD-1 MFI [mean]	1.22	2.25	1.22	2.48	0.58
% [range (mean)]	0–4(1.4%)	0–14(4.3%)	0–19(4.5%)	0–98(20.2%)	0–98(10.2%)
CTLA4 MFI [mean]	0.55	0.67	2.07	0.41	0.76
% [range (mean)]	5–9(7.5)	1–99(57.2%)	16–96(74.8%)	0–97(43.7%)	0–99(51.7%)
CD80 MFI [mean]	0.87	0.71	2.43	0.95	0.98
% [range (mean)]	0–9(7.7%)	1–99(56.2%)	14–96(74.8%)	0–98(53.7%)	0–99(56.6%)
CD86 MFI [mean]	0.09	0.16	0.28	0.26	0.19
% [range (mean)]	0–4.4(1.4%)	0–91(25.2%)	1–97(33.1%)	0–99(34.9%)	0–99(31.1%)
CD28 MFI [mean]	0.01	0.23	0.35	0.14	0.21
% [range (mean)]	0–2.4(0.8%)	0–53(13.9%)	0–63(14.8%)	0–52(8.1%)	0–63(11.6%)

Statistics

The Mann–Whitney U-test was employed to compare data. Linear correlations were estimated using Pearson's correlation. All variables were compared with age and sex. Protein expression-based heat maps and unsupervised clustering was performed by using the freely available Heatmapper online tool http://www.heatmapper.ca[31] employing the average linkage

clustering method. The seven most significant clusters according to the hierarchical clustering analysis visualized by the dendrogram were used for downstream analysis of the TME. Survival analyses were performed on 216 patients (follow-up time 36 months) using Kaplan–Meier estimators, log-rank tests and univariate and multivariate cox regression models. *p* values < 0.05 were considered statistically significant. Figures were generated using the GraphPad Prism 7.0 software, IBM SPSS Statistics 28.0 and Heatmapper (http://www.heatmapper.ca).

Data availability statement

The data generated in this study are available upon request from the corresponding author.

Results

Clinical characteristics and mutational profile

In this study, 106 MDS, 36 CMML and 132 sAML patients were analyzed regarding their survival rate and the prognostic value of genetic alterations. 29/142 MDS/CMML and 13/132 sAML patients were treated with HMA, respectively. Of 216 patients with known 3-year survival, the prognosis of the MN subgroups differed with sAML ($n = 111$) showing an inferior survival when compared to MDS/CMML patients ($n = 105$) (HR = 1.3, Supplementary Figure S1A). All clinical and pathologic parameters of MN patients are summarized in Table 1. The mutational profile and its prognostic impact was determined in 120 MN patients using NGS panel analyses and summarized in Figure 1. Mutations and variants were detected in 91.2% of all MN patients and varied from one to seven alterations per patient. The most frequently mutated genes were *TET2* (21.8%), *ASXL1* (15.1%), *SRSF2* (15.1%) and *TP53* (14.3%). The highest mean number of mutations within one sample was detectable in CMML cases when compared to MDS and sAML. While most genetic aberrations demonstrated no association with patients' age and sex, more frequent mutations in *SRSF2* ($p = 0.044$) and a slightly higher number of mutations within one sample ($p = 0.072$) were detected in patients older than 60 years. In addition, the mutational profile was associated with the survival of MDS/CMML and sAML patients as shown in Supplementary Figure S1B-C. MDS/CMML patients with multiple gene mutations in different genes as well as patients with high-risk mutations in *TP53*, *ASXL1*, *EZH2* and *RUNX1*, which were selected based on the high prevalence in our cohort, showed a significantly worse survival when compared to patients without mutations in these genes (HR = 3.46 and HR = 2.77, respectively; Supplementary Figure S1B). In contrast, no correlation between the mutational profile and the survival of sAML patients was detected (Supplementary Figure S1C).

Differences in the immune cell infiltration, ICP expression and spatial immune cell organization between nnBM and BM of MDS, CMML and sAML patients

The immune cell composition of the microenvironment was analyzed in 324 BMBs using MSI. As representatively shown in Figure 2a, both, the frequencies and the spatial distribution of CD3$^+$CD8$^-$ T cells, CD3$^+$CD8$^+$ T cells, CD3$^+$FoxP3$^+$ regulatory T cells (Tregs), CD3$^-$MUM1$^+$ B cells/plasma cells, CD3$^+$ GrB$^+$ T cells, CD3$^-$GrB$^+$ cells, CD11c$^+$ myeloid cells (MCs), CD68$^+$CD163$^-$ M1 macrophages, CD68$^+$CD163$^+$ M2 macrophages and CD3$^-$CD56$^+$ (including CD56$^+$CD16$^+$) NK cells were determined. Moreover, the expression of different ICP molecules was determined on consecutive tissue slides for all cells, but also for cell subpopulations, including T cells and macrophages (Figure 2a). The highest expression levels of ICP molecules including PD-L1 and PD-L2 were found on neoplastic hematopoietic cells, but also on different immune cell subsets. The different tumor infiltrating immune cells (TIIC), including tumor infiltrating lymphocytes (TILs; T and B cell subpopulations), exhibited the highest mean frequencies in MDS and CMML cases (Figure 2b, Table 1). All CD3$^+$ T cell subsets, but in particular CD3$^+$CD8$^+$ and CD3$^+$GrB$^+$ T cells showed higher mean values in MDS and CMML compared to sAML and non-neoplastic BM (nnBM) (Figure 2c-d, Table 1). Moreover, the frequencies of B cells/plasma cells (Figure 2e), NK cells, Tregs, MCs and macrophages were generally higher in MDS and CMML samples when compared to nnBM, but showed equal frequencies in sAML and nnBM cases (Table 1). The spatial immune cell organization (Figure 2f) revealed a higher mean distance of CD3$^+$CD8$^-$ and CD3$^+$CD8$^+$ in sAML (85.8 μm) samples when compared with nnBM and MDS/CMML (45.9 μm; 45.2 μm, respectively, Figure 2g). In contrast, no significant difference in the proximity of T cells and B/plasma cells was found in the respective diseases (Figure 2h). Age and sex did not significantly affect the frequency and composition of TILs (Supplementary Figure S1D).

Heterogeneous expression of immune modulatory markers in MN

Next to the immune cell infiltration, the expression of HLA-I HC and non-classical HLA-Ib molecules HLA-E, -F, and -G were analyzed by IHC (Figure 3a, Table 1). In nnBM, 49/50 samples showed a high HLA-I HC expression (H-score > 200). In contrast, in MDS, CMML and sAML cases the HLA-I HC staining varied with an in average reduced HLA-I HC expression in all MN subtypes with the lowest mean value for sAML cases (Figure 3b). Age and sex did not significantly affect the expression of HLA-I HC (Supplementary Figure S1E). However, while the mean HLA-E expression was lower in MDS, CMML and sAML, the expression of HLA-G was higher in some, but not all samples. Moreover, most ICP molecules showed a higher expression in neoplastic diseases including LAG3, PD-L1, TIM3, Gal-9, CTLA4, CD80, CD86, CD28 and CD69, but not of PD-1. The PD-L2 expression was highly variable in the BMB of the different MN tested (Table 1 and Supplementary Figure S2A).

In order to compare these results with an independent cohort, array data of CD34$^+$ BM cells of untreated MDS patients and nnBM were analyzed. As shown in Supplementary Figure S2B-C, the expression of classical HLA-I antigens, but also of non-classical HLA-G, -E and – F was downregulated in MDS
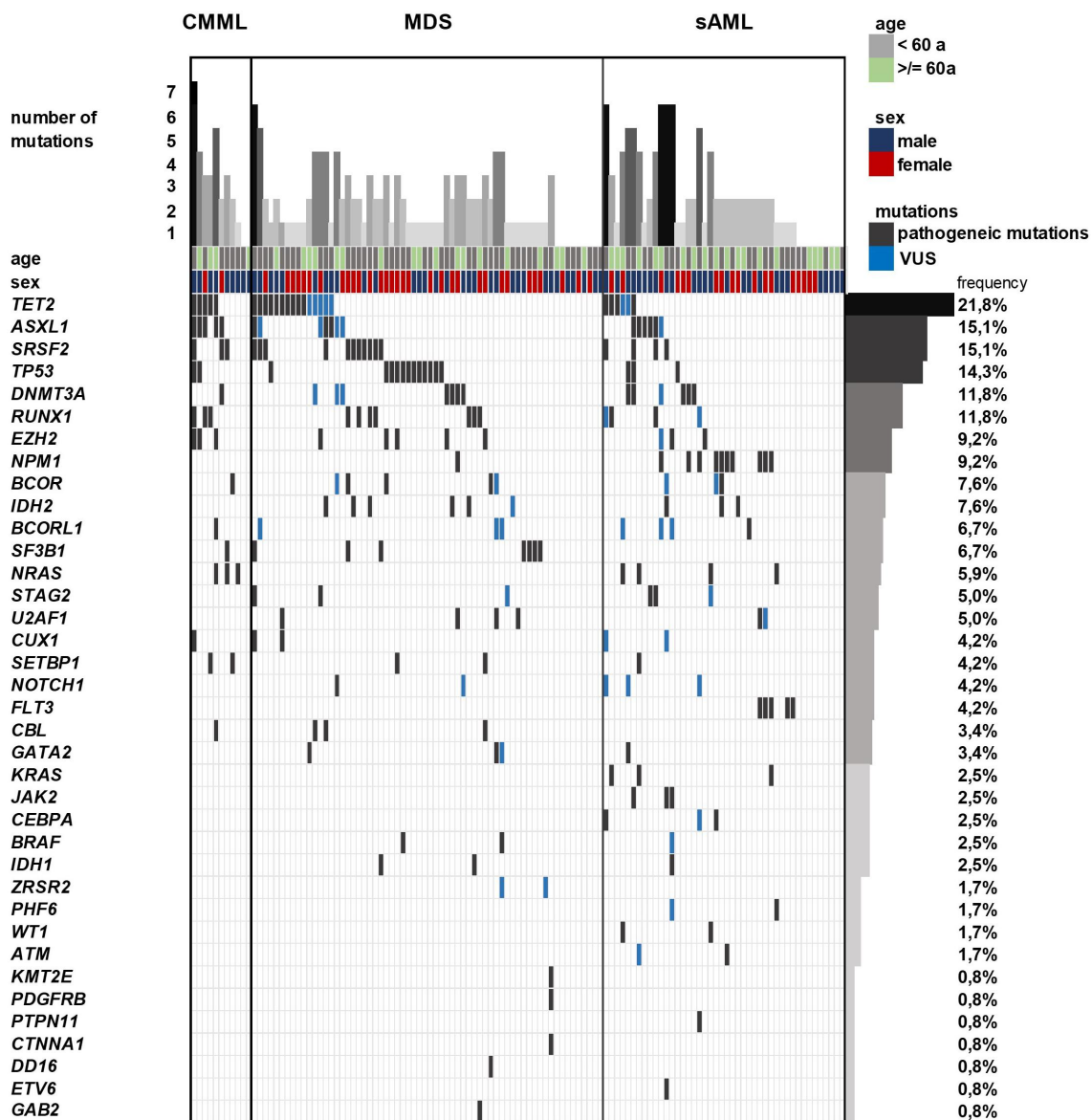
Figure 1. Mutational profiling of myeloid neoplasms (MN). the mutational profile of MDS, CMML and sAML samples was analyzed by targeted NGS. The samples are grouped by diagnosis made in comparison with clinical, genetic and histopathological features regarding the WHO classification of tumors of hematopoietic and lymphoid tissues, 4th and 5th edition. The detected pathogenic mutations are marked with black rectangles, variants of uncertain significance (VUS) with blue rectangles (nomenclature was given according to the recommendations of the Human Genome Variation Society). The age and sex of patients are marked with colored rectangles and the frequency of the respective mutated genes are shown at the right side of the graph.

samples when compared with nnBM. In line with our protein expression data, the ICP molecules analyzed showed a higher gene expression in MDS samples when compared to nnBM samples.

Influence of the distinct expression pattern on the tissue-specific immune cell composition

An unsupervised clustering analysis of HC, MDS, CMML and sAML was employed based on the expression of HLA-I, HLA-Ib as well as ICP molecules and the presence of immune cells (Figure 3c). The seven most significant clusters (C1 to C7) were selected and showed no significant differences regarding age and sex of the patients. However, the clusters with a lower expression of HLA-I HC and HLA-Ib molecules comprised the majority of sAML and MDS/CMML cases with excess of blasts (C1 and C7). In contrast, the cluster C6, characterized by a high expression of HLA-I HC, HLA-E, and HLA-F, but low HLA-G, contains most samples of HC as well as MDS and CMML cases with low blast counts. Although these clusters did not significantly differ concerning the survival (Supplementary Figure S3A), the survival analysis of sAML patients only revealed the best outcome in cluster 6 comprising most nnBM and MDS/CMML cases with low blast counts (Supplementary Figure S3B). In order to understand the link between immune cell clusters and patients' survival, the presence of different mutations was
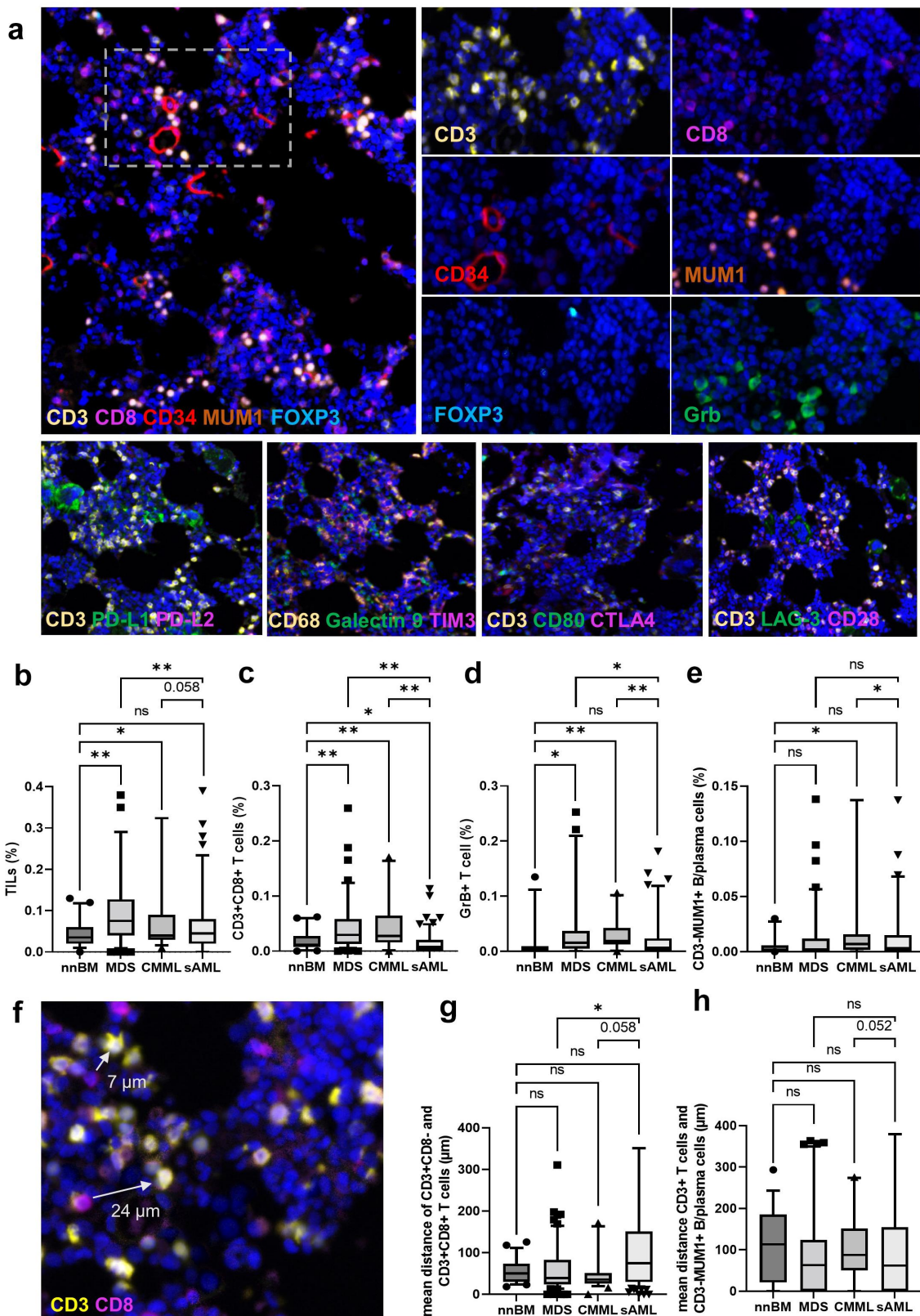
Figure 2. Distinct composition of the bone marrow microenvironment in myeloid neoplasm. Representative pictures of a multiplex IHC (a) of bone marrow (BM) from a patient with MDS with multi-lineage dysplasia (MLD) without excess of blast (EB-0) with a mutation in *SRSF2*. The amount and the composition of tissue infiltrating lymphocytes (TILs) was analyzed by MSI with a six-color Ab panel directed against CD34 (red), CD3 (yellow), CD8 (magenta), FoxP3 (cyan), MUM1p (orange), GrB (green) and counterstained with DAPI (blue). Pictures with a higher magnification of single markers combined with DAPI are shown at the right side of the picture. Consecutive slides were stained with Abs directed against PD-L1, PD-L2, gal-9, TIM3, CTLA4, CD80, CD28 and LAG3 are presented in the lower row of figure A. The immune subpopulation frequencies and intercellular distances as well as the MFI of ICP markers were assessed. Differences in the frequencies of immune cell subpopulations in 50 nnBM, 106 MDS, 36 CMML as well as 132 sAML are depicted as box plots: (b) TILs (%), (c) $CD3^+CD8^+$ T cells (%), (d) GrB^+ cells (%), and (e) $CD3^-MUM1^+$ B/plasma cells (%). (f) Representative MSI picture of a BM with $CD3^+$ (yellow) and $CD3^+CD8^+$ (yellow + magenta) T cells and their spatial relation to each other are shown. Differences in the mean spatial distance of (g) $CD3^+CD8^-$ and $CD3^+CD8^+$ T cells and (H) $CD3^+$ T cells and $CD3^-MUM1^+$ B/plasma cells are shown in box plots. Significant differences are marked with asterisks (*$p < 0.05$; **$p < 0.001$) and otherwise given with the exact p-value.
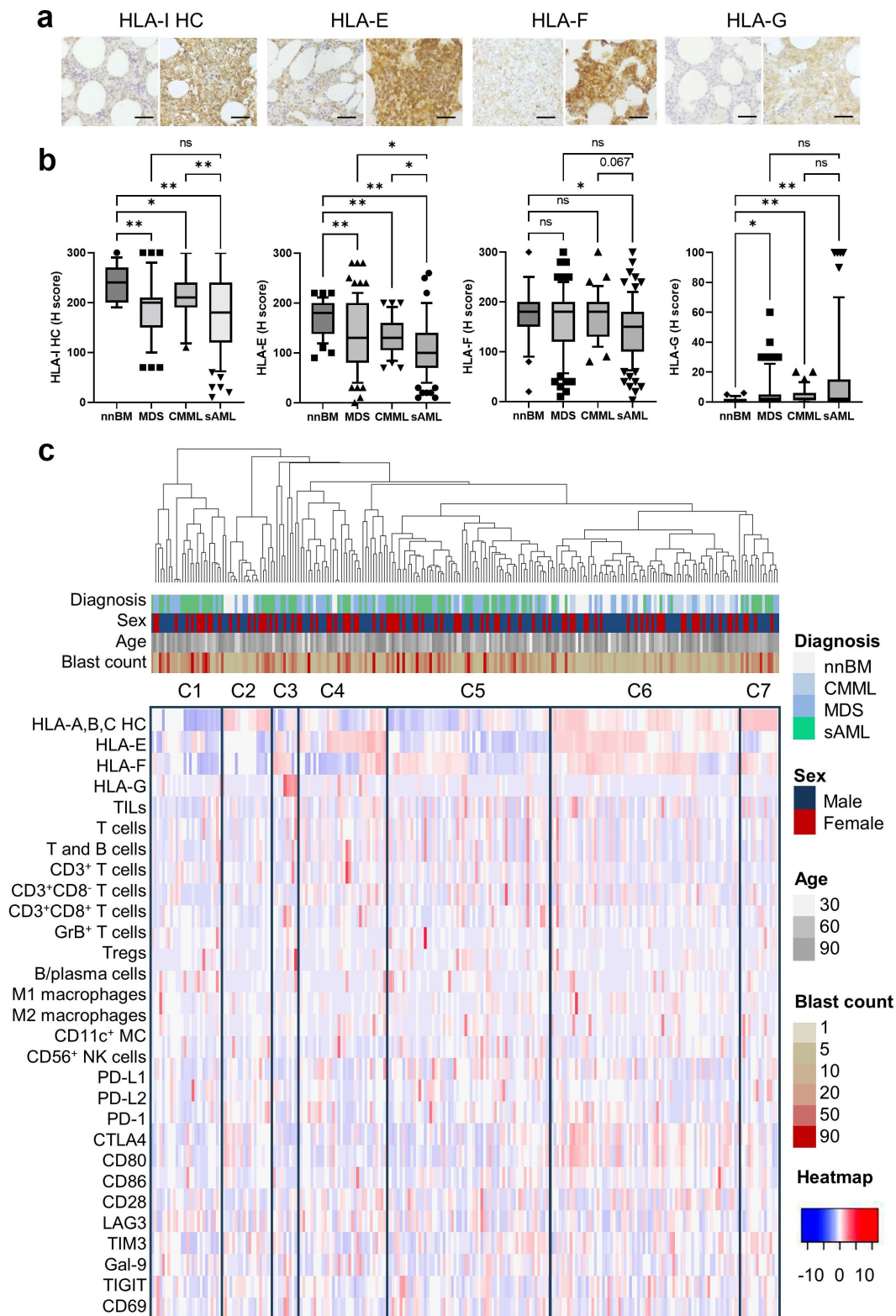
Figure 3. The immune cell infiltration, HLA-I expression and immune checkpoint (ICP) expression in the tumor microenvironment. the surface expression of different HLA-I antigens was determined by conventional IHC (a) and differences in the expression in the respective groups is depicted as box plots (b) showing HLA-A,B,C, HLA-E, HLA-F, and HLA-G. Significant differences are marked with asterisks (*$p < 0.05$; **$p < 0.001$) and otherwise given with the exact p-value. Next, HLA-I HC, HLA-Ib, ICP expression and immune cell frequencies are presented as a heat map. An unsupervised clustering of their expression was used for the TME classification. Red tiles denote increased expression, while blue tiles correspond to decreased expression (see color scheme heat map). The four horizontal bars above the heat map indicate the classification of age, sex, diagnosis (entity), and blast counts in the bone marrow.

determined in the different clusters. The prognostic worst cluster C7 showed the highest mean number of mutations per sample with a high proportion of mutations in *SRSF2*, but also in *TET2*. In contrast, the prognostic superior clusters C3 and C5 showed lower mean numbers of mutations per sample with a high frequency of *RUNX1* mutations in C3 (Supplementary Figure S3C).

Correlation of the immune landscape with the expression of immune modulatory molecules

To determine the interrelationship between the immune cell composition, HLA-Ia, HLA-Ib and ICP expression, the number of TIICs was correlated to the expression of the diverse immune modulatory molecules and mutations in MDS/CMML and sAML (Figure 4a). The frequency of TILs positively correlated with the expression of HLA-I HC and HLA-G in MDS/CMML, but inversely with LAG3 and CD28 expression. Patients with a higher TIL density showed an increased expression of cytotoxic and T cell activation markers, like GrB and CD69. However, a higher TIL density did not correlate with the proximity of T cell subpopulations. A closer proximity of CD3$^+$ and CD8$^+$ T cells was found in patients with higher HLA-I HC, CTLA4 and CD80, which was not statistically significant. In contrast, in sAML patients TILs positively correlated with CD28, but inversely with CTLA4 and CD86.

Interplay of somatic alterations and treatment with the TME

The T cell proximity was neither significantly influenced by the number of mutations per individual sample nor by the presence of high-risk mutations in MDS/CMML patients, but was associated with HLA-G and CD86 expression as well as numbers of CD8$^+$ T cells and GrB expression in sAML. However, the mutational profile inversely correlated with the number of TILs, whereby in MDS/CMML, but not in sAML patients the T cell numbers, particularly of the CD8$^+$ T cell subset, correlated with higher numbers of mutations per sample (Figure 4a,b). Furthermore, also the expression of HLA-I HC and PD-L1, but not of other molecules correlated with a higher number of mutations per sample (Figure 4b).

Next, genetic abnormalities in frequently mutated genes (*TP53*, *TET2*, *SRSF2*, and *ASXL1*) were correlated with factors in the TME as summarized in Supplementary Figure S4. In MDS/CMML patients with mutations in *TET2*, *SRSF2*, and *ASXL1* a significantly increased expression of HLA-I HC was found. In contrast, higher TIL counts only showed an association with *TP53* mutations in sAML patients.

Since epigenetic drugs are known to alter the ICP expression,[23] their influence on the expression of ICP molecules was investigated in samples from our HMA-treated patients. While in MDS, CMML and sAML patients the PD-L1 expression levels were generally higher in untreated patients when compared to HMA-treated patients, we found an upregulation of this ICP molecule in individual patients with available sequential biopsies (in total, $n = 45$ patients with sequential biopsies were available, of which 14 patients were treated with HMA before the second BMB was performed).

Individual HMA-treated patients showed a higher PD-L1 expression after HMA treatment when compared to the pre-treatment BMBs (Supplementary Figure S5A-C). Additionally, HMA-treated patients showed increased numbers of TILs including CD8$^+$ T cells that were linked with a closer T cell proximity in these patients (Supplementary Figure S3D-G). The prognostic relevance of PD-L1 was not influenced by the HMA treatment (Supplementary Figure S5H-I). Moreover, some of the patients in our cohort were treated with allogeneic stem cell transplantation (alloSCT). However, the numbers of TILs and the HLA-I HC expression showed no significant differences in patients with and without almost (Supplementary Figure S5 J-K).

Entity specific differences in the prognostic value of the TME in MDS/CMML and sAML

First, the prognostic impact of TILs was analyzed. As shown in Figure 5a,b, in MDS/CMML patients with >10% TILs (all T and B cell subsets) a significantly better survival was found when compared to those with <10% TILs (HR = 0.57). In contrast, in sAML patients no significant influence of the density of all TIICs and TILs was found (HR = 0.81). Moreover, a closer proximity of CD3$^+$CD8$^-$ and CD3$^+$CD8$^+$ T cell subsets was associated with an improved survival in MDS/CMML (HR 0.37), while no effect was found in sAML patients (Figure 5c,d). The same interrelationship was found for a higher proximity of CD3$^+$CD8$^+$ T cells and CD3$^+$FoxP3$^+$ Trigs with CD34$^+$ blasts in MDS/CMML patients, but not in sAML. However, a closer proximity of CD3$^+$FoxP3$^+$ Tregs and CD3$^+$CD8$^+$ T cells was not of clinical significance. Moreover, univariate cox regression analysis revealed that the number of mutations, presence of high-risk mutations, TIL and CD8$^+$ T cell frequency, HLA-I HC, HLA-G, PD-1, PD-L2 and CD69 expression are prognostic factors for MDS and CMML. In contrast, the survival of sAML patients was associated with HLA-I HC, PD-L1, and PD-L2 expression (for detailed information and HR see Figure 5d). Multivariate analysis demonstrated that a higher TIL frequency, closer T cell proximity and high PD-L1 expression were independent prognostic factors in MDS and CMML and correlated with superior patients' survival. In sAML patients, a higher HLA-I HC and CD28 expression were associated with increased patients' survival (Figure 5e).

Discussion

During the last decade, different genetic factors have been identified, which play a crucial role in the initiation and progression of different subtypes of MN.[5–8,10] By including the mutational profile, the predictive value of clinical risk stratification scores have even been improved.[32] In addition to tumor intrinsic factors, the TME has been defined as an important hallmark of cancer.[33] In this context, different immune cell subsets are involved in tumorigenesis by either antagonizing or promoting tumor progression.[34,35] In many solid tumors, an interrelationship between TMB and inflammation has been shown to predict the response to ICP blockade.[36] In contrast, the relatively low TMB in dnAML has been assumed to be responsible for the low efficiency of ICP blockade in this disease.[9,37,38] However, a link between immune cell infiltration and patients' outcome has been
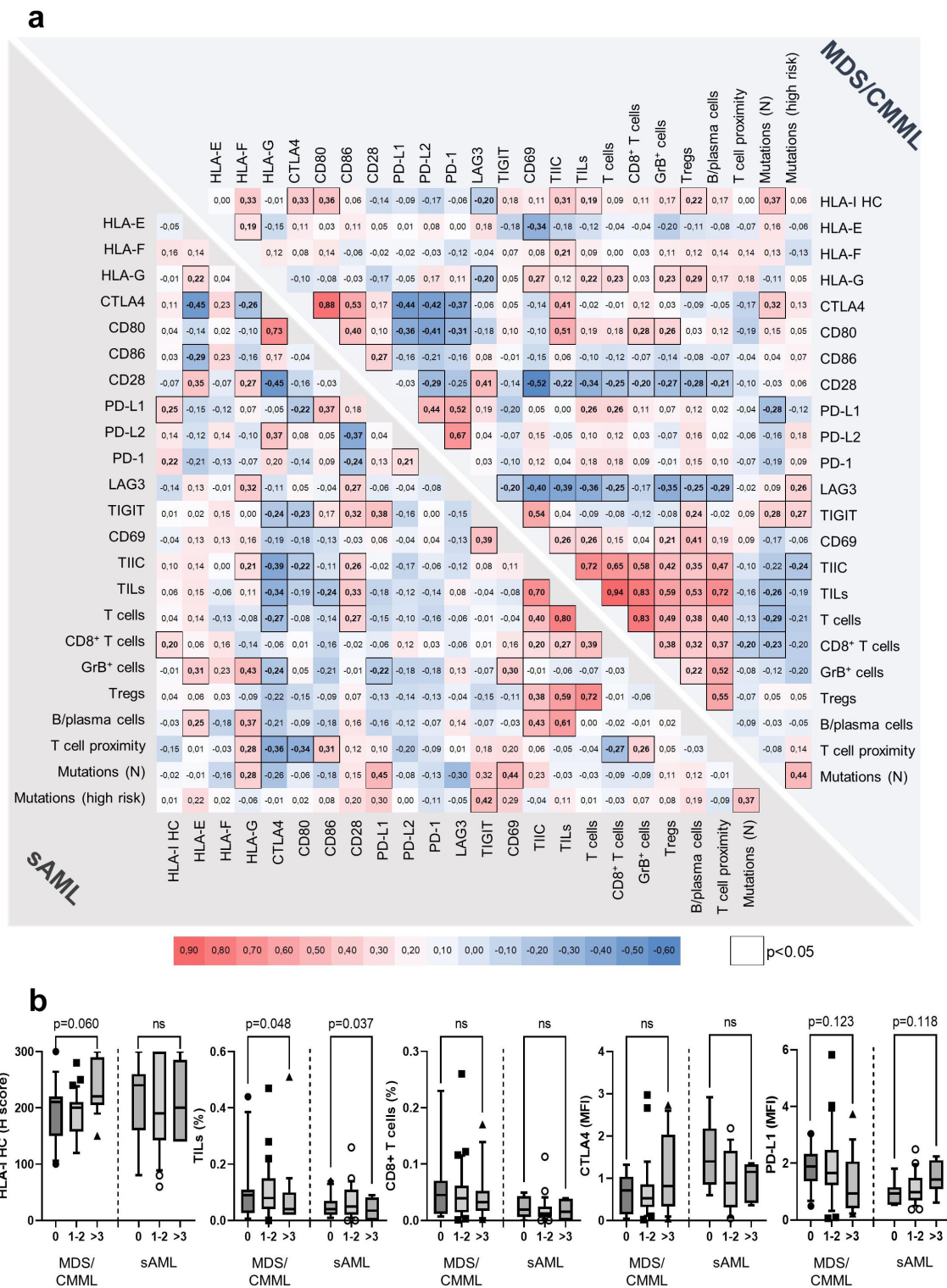
Figure 4. Complex interrelationship of immune cell composition, spatial immune cell organization, immune modulatory molecule expression, genetic aberrations and therapeutic interventions in myeloid neoplasm within the tumor microenvironment. correlation map (a) of the interplay of factors of the TME. Pearson correlation coefficients are displayed by different colors defined in the scale bar under the figure. Statistically significant correlations are highlighted with black frames. The interrelationship of number of detected mutations in individual samples is depicted with boxplots (b) concerning HLA-I HC expression, TILs, T cells and ICP expression of CTLA4 and PD-L1, was shown. Significant differences are given with the exact p-value.

demonstrated in AML cases,[13] which was influenced by *TP53* mutations.[9] So far, in MN, only limited studies investigated the relevance of ICP molecules, HLA-I and HLA-Ib expression and immune cell composition in correlation with molecular aberrations.

Using multimeric IHC, the present study showed a significant heterogeneity of the cellular immune microenvironment in MN when compared to nnBM, as also recently reported.[5,39,40] Notably, the composition, frequency and spatial distribution of different immune cell populations was
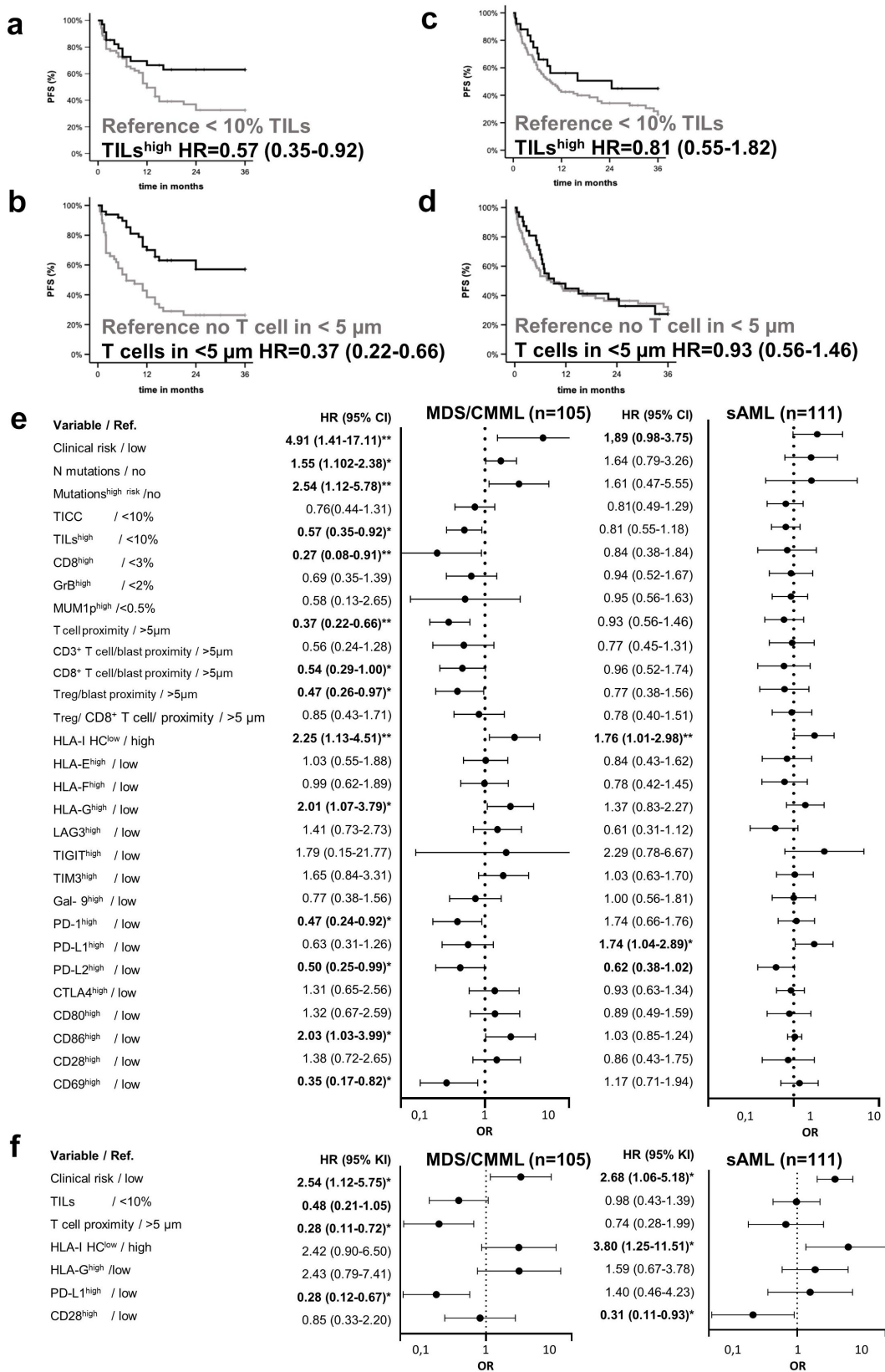
Figure 5. The prognostic impact of the tumor microenvironment in MDS/CMML and sAML. Kaplan–Meier estimators illustrate the influence of TILs and T cell densities in MDS/CMML (a-b) and sAML patients (c-d). Next, univariate cox regression analysis was performed (e) in MDS/CMML and sAML patients, respectively. Results are depicted with Forrest plots. Significant prognostic factors were further analyzed with a multivariate cox regression analysis and results are shown with Forrest plots, too (f). Significant differences are marked with asterisks ($*p < 0.05$; $**p < 0.001$).

associated with the patient´s outcome. This is in line with several studies demonstrating a prognostic impact in many human cancers[41–43] and in some subgroups of MN.[13] However, this correlation was only found in MDS and CMML patients, while in sAML, representing a continuum of these chronic myeloid neoplasms, the mean TIL frequency was significantly lower and did not affect the patients' outcome. Moreover, a closer proximity of CD3^{+} and CD8^{+} T cell subsets correlated with an improved survival in MDS and CMML, but not in sAML patients. Furthermore, the downregulation of HLA-I HC surface expression, which is a common immune escape mechanism in many malignancies,[44] showed the highest prevalence in sAML samples and correlated with an inferior survival in MDS, CMML and sAML patients. Moreover, in an unsupervised clustering model a continuum of changes in the TME composition and ICP expression was demonstrated. MDS and CMML samples with low blast counts, but also a few sAML immunologically clustered with nnBM, while other MDS and CMML cases with excess of blasts clustered with most of sAML cases. Of note, sAML patients that clustered with nnBM had an improved OS. Together, these data suggest a continuum of TME aberrations from nnBM and MDS/CCML without excess of blast to samples with increased blast counts with sAML exhibiting the most pronounced immune escape that correlated with patients´ survival. Moreover, these findings could be an explanation for the failure of ICP blockade in patients with AML.[45] Both, low TIL counts and downregulation of HLA-I have been also associated with treatment resistance in solid neoplasms.[46–48] While patients with higher TIL counts showed improved treatment effects of ICP blockade.[49] In this context, it is noteworthy that the expression of HLA-Ib molecule HLA-G might also be of prognostic relevance in MDS and CMML patients.

In order to get insights into the underlying mechanisms of the altered immune cell infiltration, mutational profiling and expression analysis of immune modulatory surface molecules was performed. The T cell infiltration and overall TIL density were inversely correlated with the number of mutations detected by NGS as described for other malignancies.[9,50] Moreover, the T cell proximity, which showed a stronger prognostic influence in multivariate cox regression when compared to TIL counts, was higher in samples with high CTLA4, CD80, HLA-I HC and higher TIL frequencies. In contrast, a higher spatial distance was found in cases with high HLA-G, TIGIT, CD69 and GrB expression.

Next, the prognostic impact of ICP expression was tested. The expression of PD-1/PD-L1/PD-L2 was associated with an improved survival in MDS and CMML suggesting a clinical relevance of this pathway. In sAML patients, a higher CD28 expression was found to be an independent prognostic marker that was associated with superior survival. These results demonstrate a unique disease specific immunological landscape with a significant prognostic impact.

Moreover, ICPs are often epigenetically controlled and it can be upregulated by HMA.[49,51–58] Furthermore, HMA have been shown to induce anti-tumor immune responses in solid tumors and hematopoietic malignancies, including MDS and sAML.[26,57] Some patients of our cohort treated with HMA exhibit differences in the expression level of several ICP molecules, with an upregulation of PD-L1 in patients after HMA treatment when compared to untreated patients. Of note, the therapeutic interventions did not change the disease-specific prognostic impact of different ICP molecules. However, it has been suggested that combinations of ICP blockade with these epigenetic drugs might be a potential efficient therapies in the MDS/sAML patients.[57,59]

Together, these data demonstrate that MDS, CMML and sAML not only differ clinically and morphologically but also regarding their immune cell composition and their expression of immune-response relevant molecules in the BM TME. This includes not only the frequency of immune cell (sub)populations but also their spatial distribution and function, which are influenced by the mutational profile, have an impact on prognosis and might serve as a target for immune-regulatory therapies. Beyond this, in a subset of MDS and CMML patients, a significant HLA-I downregulation was found and correlated with an inferior patients' survival, which was even more pronounced in sAML, and which has already been linked to ICP blockade resistance in solid tumors. Next to HLA-I this study showed for the first time a prognostic impact of the expression of non-classical HLA-G molecule. It is noteworthy that MDS and CMML diseases are also very heterogeneous and can be divided into a large number of subtypes, which cannot be fully covered in this study. In general, a strong link between the TME composition and ICP expression and the blast counts underlying the interrelationship of the neoplastic cells and the surrounding TME was reported. Despite the described interconnection of the mutational profile, the composition and spatial organization of the BM TME and immune escape mechanisms in MN, further challenges are the identification of underlying disease-subtype specific immune regulatory mechanisms in these malignancies, which yield the rational for the design of more efficient therapies and for the stratification of patients who might benefit from the respective treatment.

Abbreviations

Ab, Antibody; AML, Acute myeloid leukemia; BM, bone marrow, BMB; bone marrow biopsy; CMML, chronic myelomonocytic leukemia; CTLA4, cytotoxic T lymphocyte-associated protein 4; DGE, differentially gene expression; dnAML, de-novo AML; FFPE, formalin-fixed and paraffin-embedded; Gal-9, galectin 9; GrB, granzyme B; HC, heavy chain; HLA, human leukocyte antigen; HR, hazard ratio; ICP, immune checkpoint; LAG3, lymphocyte-activation gene 3; MC, CD11c+ myeloid cell; MDS, myelodysplastic neoplasm; MDS/MPN, myelodysplastic/

myeloproliferative neoplasm; MF, myelofibrosis; MFI, mean fluorescence intensity; MN, myeloid neoplasm; MPN, myeloproliferative neoplasm; MPO, myeloperoxidase; MSI, multispectral imaging; NGS, next generation sequencing; nnBM, non-neoplastic BM; NSCLC, non-small cell lung cancer; OS, overall survival; PD-1, programmed cell death receptor 1; PD-L1, programmed death ligand 1; PFS, progression-free survival; sAML, secondary AML; TCGA, The Cancer Genome Atlas; TIGIT, T cell immunoreceptor with Ig and ITIM domains; TIIC, tumor infiltrating immune cells; TIL, tumor infiltrating lymphocyte; TIM3, T cell immunoglobulin and mucin-domain containing-3; TMB, tumor mutational burden; TME, tumor microenvironment; Treg, CD3$^+$FoxP3$^+$ regulatory T cells; TSA, tyramide signal amplification; WHO, World Health Organization.

Author contributions

References

1. Arber DA, Orazi A, Hasserjian R, Thiele J, Borowitz MJ, Le Beau MM, Bloomfield CD, Cazzola M, Vardiman JW. International consensus classification of myeloid neoplasms and acute leukemias: integrating morphologic, clinical, and genomic data. Blood. 2022 Sep 15;140(11):1200–1228. doi:10.1182/blood.2022015850.

2. Arber DA, Orazi A, Hasserjian R, Thiele J, Borowitz ML, Le Beau MM, Bloomfield CD, Cazzola M, Vardiman JW. The 2016 revision to the World Health Organization classification of myeloid neoplasms and acute leukemia. Blood. 2016 May 19;127 (20):2391–2405. doi:10.1182/blood-2016-03-643544.

3. Miesner M, Haferlach C, Bacher U. et al. Multilineage dysplasia (MLD) in acute myeloid leukemia (AML) correlates with MDS-related cytogenetic abnormalities and a prior history of MDS or MDS/MPN but has no independent prognostic relevance: a comparison of 408 cases classified as "AML not otherwise specified" (AML-NOS) or "AML with myelodysplasia-related changes" (AML-MRC). Blood. 2010 Oct 14;116(15):2742–2751. doi:10.1182/blood-2010-04-279794.

4. Goel H, Rahul E, Gupta I. et al. Molecular and genomic landscapes in secondary & therapy related acute myeloid leukemia. Am J Blood Res. 2021;11(5):472–497.

5. Bauer M, Vaxevanis C, Al-Ali HK. et al. Altered spatial composition of the Immune Cell Repertoire in Association to CD34+ blasts in myelodysplastic syndromes and secondary acute myeloid leukemia. Cancers. 2021 Jan 7;13(2):186. doi:10.3390/cancers13020186.

6. Ivy KS, Brent Ferrell P. Disordered Immune Regulation and its therapeutic targeting in myelodysplastic syndromes. Curr Hematol Malig Rep. 2018;13(4):244–255. doi:10.1007/s11899-018-0463-9.

7. Sallman DA, List A. The central role of inflammatory signaling in the pathogenesis of myelodysplastic syndromes. Blood. 2019 Mar 7; 133(10):1039–1048. doi:10.1182/blood-2018-10-844654.

8. Fisher DAC, Fowles JS, Zhou A, Oh ST. Inflammatory pathophysiology as a contributor to Myeloproliferative Neoplasms. Front Immunol. 2021;12:683401. doi:10.3389/fimmu.2021.683401.

9. Wen XM, Xu ZJ, Jin Y. et al. Association analyses of TP53 mutation with prognosis, tumor mutational burden, and immunological features in acute myeloid leukemia. Front Immunol. 2021;12:717527. doi:10.3389/fimmu.2021.717527.

10. Sallman DA, Komrokji R, Vaupel C. et al. Impact of TP53 mutation variant allele frequency on phenotype and outcomes in myelodysplastic syndromes. Leukemia. 2016 Mar;30(3):666–673. doi:10.1038/leu.2015.304.

11. Bewersdorf JP, Hasle V, Shallis RM. et al. Molecular, Epigenetic, and Immune Landscape of TP53- mutated (TP53-M) Acute Myeloid Leukemia (AML) and Higher Risk Myelodysplastic Syndromes (HR-MDS). Blood. 2022 Nov 15;140(Supplement 1):6247–6249. doi:10.1182/blood-2022-156460.

12. Bewersdorf JP, Xie Z, Bejar R. et al. Current landscape of translational and clinical research in myelodysplastic syndromes/neoplasms (MDS): proceedings from the 1st International Workshop on MDS (iwMDS) of the International consortium for MDS (icMDS). Blood Rev. 2023 Jul;60:101072. doi:10.1016/j.blre.2023.101072.

13. Vadakekolathu J, Minden MD, Hood T. et al. Immune landscapes predict chemotherapy resistance and immunotherapy response in acute myeloid leukemia. Sci Transl Med. 2020 Jun 3;12(546):eaaz0463. doi:10.1126/scitranslmed.aaz0463.

14. Lasry A, Nadorp B, Fornerod M. et al. An inflammatory state remodels the immune microenvironment and improves risk stratification in acute myeloid leukemia. Nat Cancer [Internet]. 2022 Dec 29 [cited 2023 Apr 24]. doi:10.1038/s43018-022-00480-0.

15. Rutella S, Vadakekolathu J, Mazziotta F. et al. Immune dysfunction signatures predict outcomes and define checkpoint blockade–unresponsive microenvironments in acute myeloid leukemia. J Clin Invest. 2022 Nov 1;132(21):e159579. doi:10.1172/JCI159579.

16. Masters SL, Gerlic M, Metcalf D. et al. NLRP1 inflammasome activation induces pyroptosis of hematopoietic progenitor cells. Immunity. 2012 Dec 14;37(6):1009–1023. doi:10.1016/j.immuni.2012.08.027.

17. Moiseev I, Tcvetkov N, Epifanovskaya O. et al. Landscape of alterations in the checkpoint system in myelodysplastic syndrome and implications for prognosis. PLoS One. 2022;17(10):e0275399. doi:10.1371/journal.pone.0275399.

18. Sallman DA, McLemore AF, Aldrich AL. et al. TP53 mutations in myelodysplastic syndromes and secondary AML confer an immunosuppressive phenotype. Blood. 2020 Jul 30;136(24):2812–2823. doi:10.1182/blood.2020006158.

19. Lübbert M, Suciu S, Baila L. et al. Low-dose decitabine versus best supportive care in elderly patients with intermediate- or high-risk myelodysplastic syndrome (MDS) ineligible for intensive chemotherapy: final results of the randomized phase III study of the European Organisation for Research and Treatment of Cancer Leukemia Group and the German MDS study Group. J Clin Oncol Off J Am Soc Clin Oncol. 2011 May 20;29 (15):1987–1996.

20. Kantarjian HM, Thomas XG, Dmoszynska A. et al. Multicenter, randomized, open-label, phase III trial of decitabine versus patient choice, with physician advice, of either supportive care or low-dose cytarabine for the treatment of older patients with newly diagnosed acute myeloid leukemia. J Clin Oncol Off J Am Soc Clin Oncol. 2012 Jul 20;30(21):2670–2677. doi:10.1200/JCO.2011.38.9429.

21. Fenaux P, Mufti GJ, Hellstrom-Lindberg E. et al. Efficacy of azacitidine compared with that of conventional care regimens in the treatment of higher-risk myelodysplastic syndromes: a randomised, open-label, phase III study. Lancet Oncol. 2009 Mar;10(3):223–232. doi:10.1016/S1470-2045(09)70003-8.

22. Qiu X, Hother C, Ralfkiær UM. et al. Equitoxic doses of 5-azacytidine and 5-aza-2'deoxycytidine induce diverse immediate and overlapping heritable changes in the transcriptome. PLoS One. 2010 Sep 29;5(9):e12994. doi:10.1371/journal.pone.0012994.

23. Ørskov AD, Treppendahl MB, Skovbo A. et al. Hypomethylation and up-regulation of PD-1 in T cells by azacytidine in MDS/AML patients: a rationale for combined targeting of PD-1 and DNA methylation. Oncotarget. 2015 Apr 20;6(11):9612–9626. doi:10.18632/oncotarget.3324.

24. Youngblood B, Oestreich KJ, Ha SJ. et al. Chronic virus infection enforces demethylation of the locus that encodes PD-1 in antigen-specific CD8(+) T cells. Immunity. 2011 Sep 23;35 (3):400–412. doi:10.1016/j.immuni.2011.06.015.

25. Klümper N, Ralser DJ, Bawden EG. et al. LAG3 (LAG-3, CD223) DNA methylation correlates with LAG3 expression by tumor and immune cells, immune cell infiltration, and overall survival in clear cell renal cell carcinoma. J Immunother Cancer. 2020 Mar;8(1):e000552. doi:10.1136/jitc-2020-000552.

26. Daver N, Boddu P, Garcia-Manero G. et al. Hypomethylating agents in combination with immune checkpoint inhibitors in acute myeloid leukemia and myelodysplastic syndromes. Leukemia. 2018 May;32 (5):1094–1105. doi:10.1038/s41375-018-0070-8.

27. Weltgesundheitsorganisation. WHO classification of tumours of haematopoietic and lymphoid tissues. In: Swerdlow S, Campo E, Harris N, Jaffe E, Pileri S, Stein H. editor(s). World Health Organization classification of tumours. Revised 4th edition. Lyon: International Agency for Research on Cancer;2017p. 585.

28. Editorial Board. WHO classification of tumours editorial board. Haematolymphoid tumours [Internet; beta version ahead of print]. Lyon (France): International Agency for Research on Cancer; 2022 cited 2023-03-10. (WHO classification of tumours series, 5th ed.; vol. 11).

29. Bauer M, Vaxevanis C, Bethmann D. et al. Multiplex immunohistochemistry as a novel tool for the topographic assessment of the bone marrow stem cell niche. Methods Enzymol. 2020;635:67–79.

30. Graubert TA, Shen D, Ding L. et al. Recurrent mutations in the U2AF1 splicing factor in myelodysplastic syndromes. Nat Genet. 2011 Dec 11;44(1):53–57. doi:10.1038/ng.1031.

31. Babicki S, Arndt D, Marcu A. et al. Heatmapper: web-enabled heat mapping for all. Nucleic Acids Res. 2016 Jul 8;44(W1): W147–53. doi:10.1093/nar/gkw419.

32. Gu S, Xia J, Tian Y. A novel scoring system integrating molecular abnormalities with IPSS-R can improve the risk stratification in patients with MDS. BMC Cancer. 2021 Feb 6; 21(1):134. doi:10. 1186/s12885-021-07864-y.

33. Hanahan D. Hallmarks of cancer: new dimensions. Cancer Discov. 2022 Jan;12(1):31–46. doi:10.1158/2159-8290.CD-21-1059.

34. Bauer M, Jasinski-Bergner S, Mandelboim O. Epstein-Barr Virus-Associated Malignancies and immune escape: the role of the tumor microenvironment and tumor cell evasion strategies. Cancers. 2021 Oct 16; 13(20):5189. doi:10.3390/cancers13205189.

35. Wickenhauser C, Bethmann D, Kappler M. et al. Tumor microenvironment, HLA class I and APM expression in HPV-Negative oral squamous cell carcinoma. Cancers. 2021 Feb 4;13(4):620. doi:10.3390/cancers13040620.

36. Samstein RM, Lee CH, Shoushtari AN. et al. Tumor mutational load predicts survival after immunotherapy across multiple cancer types. Nat Genet. 2019 Feb;51(2):202–206. doi:10.1038/s41588-018-0312-8.

37. Lawrence MS, Stojanov P, Polak P. et al. Mutational heterogeneity in cancer and the search for new cancer-associated genes. Nature. 2013 Jul 11;499(7457):214–218. doi:10.1038/nature12213.

38. Stahl M, Goldberg AD. Immune checkpoint inhibitors in acute myeloid leukemia: novel combinations and therapeutic targets. Curr Oncol Rep. 2019 Mar 23; 21(4):37. doi:10.1007/s11912-019-0781-7.

39. Kordasti SY, Afzali B, Lim Z. et al. IL-17-producing CD4(+) T cells, pro-inflammatory cytokines and apoptosis are increased in low risk myelodysplastic syndrome. Br J Haematol. 2009 Apr;145 (1):64–72. doi:10.1111/j.1365-2141.2009.07593.x.

40. Lopes MR, Traina F, de M CP. et al. IL10 inversely correlates with the percentage of CD8+ cells in MDS patients. Leuk Res. 2013 May;37(5):541–546. doi:10.1016/j.leukres.2013.01.019.

41. Galon J, Costes A, Sanchez-Cabo F. et al. Type, density, and location of immune cells within human colorectal tumors predict clinical outcome. Science. 2006 Sep 29;313(5795):1960–1964. doi:10.1126/science.1129139.

42. Salgado R, Denkert C, Demaria S. et al. The evaluation of tumor-infiltrating lymphocytes (TILs) in breast cancer: recommendations by an international TILs working group 2014. Ann Oncol. 2015 Feb;26(2):259–271. doi:10.1093/annonc/mdu450.

43. Ding R, Prasanna P, Corredor G. et al. Image analysis reveals molecularly distinct patterns of TILs in NSCLC associated with treatment outcome. NPJ Precis Oncol. 2022 Jun 3;6(1):33. doi:10. 1038/s41698-022-00277-5.

44. Dhatchinamoorthy K, Colbert JD, Rock KL. Cancer Immune Evasion Through Loss of MHC class I antigen presentation. Front Immunol. 2021;12:636568. doi:10.3389/fimmu.2021. 636568.

45. Boddu P, Kantarjian H, Garcia-Manero G. The emerging role of immune checkpoint based approaches in AML and MDS. Leuk Lymphoma. 2018 Apr;59(4):790–802. doi:10.1080/10428194.2017. 1344905.

46. Lee JH, Shklovskaya E, Lim SY. et al. Transcriptional downregulation of MHC class I and melanoma de- differentiation in resistance to PD-1 inhibition. Nat Commun. 2020 Apr 20;11(1):1897. doi:10. 1038/s41467-020-15726-7.

47. Lei Q, Wang D, Sun K. Resistance mechanisms of anti-PD1/PDL1 therapy in solid tumors. Front Cell Dev Biol. 2020;8:672. doi:10. 3389/fcell.2020.00672.

48. Kuba K, Inoue H, Matsumura S. et al. A retrospective analysis of tumor infiltrating lymphocytes in head and neck squamous cell carcinoma patients treated with nivolumab. Sci Rep. 2022 Dec 29;12(1):22557. doi:10.1038/s41598-022-27237-0.

49. Penter L, Liu Y, Wolff JO. et al. Mechanisms of response and resistance to combined decitabine and ipilimumab for advanced myeloid disease. Blood. 2023 Jan 27. 2022018246.

50. Wang X, Li M. Correlate tumor mutation burden with immune signatures in human cancers. BMC Immunol. 2019 Jan 11; 20(1):4. doi:10.1186/s12865-018-0285-5.

51. Griffiths EA, Srivastava P, Matsuzaki J. et al. NY-ESO-1 vaccination in combination with Decitabine Induces Antigen-Specific T-lymphocyte Responses in patients with myelodysplastic syndrome. Clin Cancer Res Off J Am Assoc Cancer Res. 2018 Mar 1;24(5):1019–1029. doi:10.1158/1078-0432.CCR-17-1792.

52. Abaza Y, Zeidan AM. Immune checkpoint inhibition in acute myeloid leukemia and myelodysplastic syndromes. Cells. 2022 Jul 20; 11(14):2249. doi:10.3390/cells11142249.

53. Wong KK, Hassan R, Yaacob NS. Hypomethylating agents and immunotherapy: Therapeutic Synergism in acute myeloid leukemia and myelodysplastic syndromes. Front Oncol. 2021;11:624742. doi:10.3389/fonc.2021.624742.

54. Serrano A, Castro-Vega I, Redondo M. Role of gene methylation in antitumor immune response: implication for tumor progression. Cancers. 2011 Mar 29; 3(2):1672–1690. doi:10.3390/cancers3021672.

55. Nangalia J, Grinfeld J, Green AR. Pathogenesis of myeloproliferative disorders. Annu Rev Pathol. 2016 May 23; 11(1):101–126. doi:10.1146/annurev-pathol-012615-044454.

56. Yang G, Wang X, Huang S. et al. Generalist in allogeneic hematopoietic stem cell transplantation for MDS or AML: epigenetic therapy. Front Immunol. 2022;13:1034438. doi:10.3389/fimmu. 2022.1034438.

57. Yang H, Bueso-Ramos C, DiNardo C. et al. Expression of PD-L1, PD-L2, PD-1 and CTLA4 in myelodysplastic syndromes is enhanced by treatment with hypomethylating agents. Leukemia. 2014 Jun;28(6):1280–1288. doi:10.1038/leu.2013.355.

58. Yang X, Ma L, Zhang X. Targeting PD-1/PD-L1 pathway in myelodysplastic syndromes and acute myeloid leukemia. Exp Hematol Oncol. 2022 Mar 2; 11(1):11. doi:10.1186/s40164-022-00263-4.

59. Saxena K, Herbrich SM, Pemmaraju N. et al. A phase 1b/2 study of azacitidine with PD-L1 antibody avelumab in relapsed/ refractory acute myeloid leukemia. Cancer. 2021 Oct 15;127 (20):3761–3771. doi:10.1002/cncr.33690.